Impact of ice-free oases on particulate matter over the East Antarctic: Inferences from the carbonaceous, water-soluble species and trace metals

Suresh K R Boreddy, Prashant Hegde, A.R. Aswini, I.A. Girach, N. Koushik, K. Nalini

Polar Science 24 (2020) 100520

Contents lists available at ScienceDirect

Polar Science

journal homepage: http://www.elsevier.com/locate/polar

Impact of ice-free oases on particulate matter over the East Antarctic: Inferences from the carbonaceous, water-soluble species and trace metals

Suresh K.R. Boreddy, Prashant Hegde *, A.R. Aswini, I.A. Girach, N. Koushik, K. Nalini [1]

Space Physics Laboratory, Vikram Sarabhai Space Centre, Thiruvananthapuram, 695022, India

ARTICLE INFO

Keywords:
PM_{10}
Ice-free regions
East Antarctica
HTAs
LTAs

ABSTRACT

The present study reports on carbonaceous, water-soluble species and trace metals in PM_{10} aerosols collected at Bharati station during the austral summer (December 17, 2016 to February 2, 2017) over East Antarctica. Organic matter was the predominant among all measured species followed by nss-Ca^{2+} and nss-SO_4^{2-}. Two distinct air masses that arrive from high-altitude-troposphere (HTAs) and low-altitude-troposphere (LTAs) regions which clearly showed significant differences in concentrations of measured chemical and metal species as inferred from the air mass backward trajectory analysis and mixed layer height variations. Based on significant positive correlations among chemical species, aerosol liquid water content (ALWC), and PM_{10} mass, we confirmed that the aqueous-phase formation of secondary aerosols followed by atmospheric processing are possible sources in HTAs while primary emissions associated with soil/dust from ice-free regions and *in-situ* emissions are major sources in LTAs. This result further supported by significant ($p < 0.05$) higher concentrations of specific trace metals (for example, Fe, Ti, and Pb) in LTAs. Moreover, higher cation-to-anion (Σ^+/Σ^-) ratios suggesting the alkaline nature of aerosols at Bharati. The present study demonstrates that ice-free regions over East Antarctica may act as major sources of particulate matter, thus significant implications toward climate change over the global environment.

1. Introduction

Antarctica is traditionally considered as one of the major pristine environments on Earth, which provide an ideal place to study the background aerosol processes and its biogeochemical chemistry in the atmosphere. It is moreover useful to comprehend the influence of local atmospheric conditions and long-range transport of various chemical/physical transformations in the pristine atmosphere (Shaw, 1988). Ice-core or sediment studies which are very helpful to infer the past atmospheric information, are largely dependent on the aerosols' chemical/elemental composition in the Antarctic region because it can assist to define whether they are associated with natural or anthropogenic origin (Bao et al., 2000; Hodgson et al., 2004; Mayewski et al., 2009). Therefore, understanding the chemical and metal composition of Antarctic aerosols are crucial and one of the major points in polar research.

The particulate matter in the Antarctic atmosphere mostly composed of OM (organic matter), non sea-salt sulfate (nss-SO_4^{2-}), sea-salt (Na^+ and Cl^-), and mineral dust (Ali et al., 2015; Barbaro et al., 2016; Budhavant et al., 2016; Du et al., 2018; Giordano et al., 2017; Hara et al., 2004; Legrand et al., 2017; Lim et al., 2019; Weller et al., 2011). During the austral summer (December to March), the oceans around Antarctica release a huge amounts of various chemical compounds to the atmosphere (Quinn and Bates, 2011; Shaw, 1988; Weller et al., 2018). In addition to primary sea-salts, secondary formation of sulfur containing aerosols (nssSO_4^{2-} and MSA^-) over the oceans can be transported to continental Antarctica and ultimately deposited on the ice shield. It is suggested that nss-SO_4^{2-} and MSA^- over Antarctic comes from the biogenic activity in the oceanic surface in summer (Legrand et al., 2001; Quinn and Bates, 2011). The heterogeneous reactions involving DMS emitted by marine phytoplankton may be the dominant source of biogenic nss-SO_4^{2-} and MSA^- in the Antarctic troposphere (Giordano et al., 2017; Kreidenweis and Seinfeld, 1988; Read et al., 2008; Weller et al., 2008). High inland soils may also significant sources of nss-SO_4^{2-} in the Antarctic near surface atmosphere (Bao et al., 2000). Chloride loss in summer at the coastal Antarctic locations has been reported elsewhere (Jourdain and Legrand, 2002; Kerminen et al., 2000; Legrand et al., 2017). Oceans can also emit both primary and secondary organic

* Corresponding author.
E-mail addresses: hegdeprashant@yahoo.com, prashant_hegde@vssc.gov.in (P. Hegde).
[1] Present address: Laboratoire des sciences du climat et de l'environnement, GIF-sur-Yvette 91190, France.

https://doi.org/10.1016/j.polar.2020.100520
Received 17 August 2019; Received in revised form 29 November 2019; Accepted 21 February 2020
Available online 24 February 2020

particles (Boreddy et al., 2018; Jung et al., 2019; Kawamura et al., 1996; Lim et al., 2019; Liu et al., 2018; Virkkula et al., 2006). Carbonaceous particles, for example elemental carbon (EC, a strong light-absorber), primarily emitted by fossil-fuel and biomass burning combustion. It can transport to long distances over the globe and recognized as a significant contributor to hasten the snow/ice melt (Xu et al., 2016). All these chemical species may have an effect on climate directly (by absorbing and scattering solar radiation) and indirectly (by modifying the cloud properties, for example, refractive index, lifetime) thus precipitation pattern (Ayers and Gras, 1991; Meskhidze and Nenes, 2006).

Antarctic region is the largest polar desert over the globe and has approximately about 2% of its surface area as ice-free which is often referred as ice-free oases. Apart from fluvial activities, aeolian transport (soil erosion) is the salient processes of ice-free oases owing to its prevailing strong katabatic winds (Bullard et al., 2016; Shi et al., 2015). Bullard et al. (2016) reported that ice-free oases in the Antarctica continent act as active dust sources (Kavan and Nyvlt, 2018) which significantly reduce the precipitation over this region ranging between 3 and 50 mm/yr on a annual mean scale (Fountain et al., 2009; van Lipzig et al., 2004). Bory et al. (2010) reported that ice-free regions over the East Antarctica (EA) contain many active dust sources as inferred from snow-pits analysis at Berkner Island. Further, coastal ice-free oases can also recognize as relatively major dust sources around the Maitri, Larsemann Hills (LH), and Neumayer Station over the EA region (Budhavant et al., 2015; Chaubey et al., 2011; Weller et al., 2008). Human influence is one of the effects that change the levels of trace metals. Literature studies suggested that both terrestrial and marine environments are getting contaminated due to persistent organic pollutants (POPs) as well as trace metals in Antarctica (Bargagli et al., 2005, 2007). It is further suggested that anthropogenic sources that associated with human influence are major contributors of Pb concentrations in Antarctic snow (Hong et al., 2002). The dominant trace metals in Antarctic soil were Al, Ca, Cd, Cr and Cu (Lu et al., 2012). Because of the human activities in the surrounding areas of research stations and the prevailing wind conditions, the soil dust enters into the atmosphere and even get transported to far-off regions through global circulations (Lu et al., 2012; Potapowicz et al., 2019). Al, Fe, Ti, and Ca can be considered as natural origin (Szopinska et al., 2018) while fuel combustions are the most important sources of many trace metals including Pb, Cr, Cd and V over the Antarctic environment (Santos et al., 2005). However, none of the studies have dealt with in a systematic way on how these ice-free oases influence the atmospheric particulate composition and consequently climate over the EA.

Larsemann Hills (LHs), situated in the Indian Ocean sector, is the second largest ice-free oasis along the coast of EA occupied approximately an area of 50 km^2. It is consisting of low rounded hills alongside the southeastern coast of Prydz Bay. During the austral summer, this area experiences strong katabatic winds that blow from east to southeast confining frequently over the coastal belt of Antarctic sub-continent (Nylen et al., 2004). Several research stations (Bharati, Law base, Progress, and Zhongshan) have been established by different countries (India, Australia, Russia and China) to study the Antarctic climatology of aerosols and its changes concerning the local atmospheric conditions and anthropogenic influences. Even though many studies were done on the physical characterization of aerosols and their sources in LHs (Ali et al., 2015; Budhavant et al., 2015; Chaubey et al., 2011; Gogoi et al., 2018), still there is a knowledge gap in finding the accurate sources and nature of aerosols. For instance, Ali et al. (2015) reported low mass loadings of TSPs in LHs and found them to be mostly acidic in nature. In contrast, Xu et al. (2018) investigated chemical and elemental compositions of bulk aerosols at the Chinese Zhongshan Station in EA and reported that atmospheric aerosols in EA are not that acidic in the austral summer. Further, studies on carbonaceous aerosols and their sources and formation mechanisms are sparse over the EA, particularly in LHs.

In this study, we report a comprehensive picture on the chemical characterization and elemental composition of Antarctic aerosols including the carbonaceous components, water-soluble ionic composition, and metallic species (elemental composition) in PM_{10} aerosols that were collected at Bharati in EA during austral summer. We discuss the changes in mass concentrations of measured chemical species with respect to changes in air mass origins and mixing levels in the atmosphere. Sources of elemental composition using some tracer metal compounds are also addressed to better study the natural and geochemical variability of soils of ice-free regions in EA. Results for aerosol liquid water content (ALWC) and acidity are of interest here to discuss the aqueous-phase formation and nature of atmospheric aerosols in EA. Finally, significant climatic implications are discussed briefly based on the inferences from this study.

2. Method

2.1. Sampling site and general meteorology

As a part of 36th ISEA (Indian Scientific Expedition to Antarctica) and SPL (Space Physics Laboratory)'s polar research program, aerosol sampling was conducted at Bharati (69.40° S; 76.19° E). The sampling site, Bharati, is situated in Broknes peninsula in the LHs, over the EA about 3500 km east of Maitri, and very near to the open ocean at a lower elevation of ~40 m above sea level (see Fig. 1). However, other scientific bases by Australia (Law), Russia (Progress I and II), and China (Zhongshan) situated around 10 km away in a northeast direction from the sampling site. All these research stations are placed within a radius of 2.5 km from each other (Figure S1). Ice-free regions around Bharati were also shown in Figure S1. This geographical setting is thus favorable for being influenced by local winds.

Meteorological parameters such as wind speed (WS, ms^{-1}), wind direction (WD, Deg), air temperature (Temp, °C) and relative humidity (RH, %) are very crucial to discuss the possible sources, formation processes, and transport pathways of atmospheric aerosol particles under various atmospheric conditions. Fig. 2 illustrates the hourly variations of meteorological parameters recorded at Bharati by the Indian meteorological department (IMD) during the study period. As seen from Fig. 2, the wind speeds were ranged 0.5–15.8 ms^{-1} (mean: 5.04 ± 0.11 ms^{-1}) and northeast and easterly (45°–90°) winds are dominated. The air temperatures were ranged from −4.18 to 8.05 °C with a mean of 1.88 ± 1.40 °C while RH varied between 42 and 94% (54.1 ± 1.2%). The temporal trend of air temperature showed significant ($p < 0.05$) higher values during the first half compared to those during the second half of the sampling period (Fig. 2).

2.2. Aerosol sampling

PM_{10} samples were collected on quartz microfiber filters (Whatman, 203 mm × 254 mm; pre-combusted at 450 °C for 6 h) using a high volume sampler (HVS, APM 460 BL of Envirotech Instruments Pvt. Ltd., India) at Bharati during the period from December 17, 2016 to February 2, 2017. The sampling duration was about 12–23 h. The HVS was switched off due to the local anthropogenic activities in the vicinity of sampling location, as a result a wide spread in the sampling duration. A total of 34 aerosol and 3 field blank filters were collected in the complete study period. The field blanks (background aerosol concentrations) were collected by loading a pre-combusted filter on the sampling head for 10–15 min under the absence of pump running. The HVS was operated at a fixed flow rate of ~1 m^3 min^{-1} and the sampled total air volumes ranged between 734 and 1560 m^3 (mean: 1045 ± 360 m^3). Air volumes were estimated using the flow rate and sampling duration (min). The sampler was calibrated prior to the experiment and air flow was monitored and recorded while sampling. After collection, the filters were enfolded with a clean aluminium foils and then put in a zip-lock bags. All these samples were shipped in a refrigerated container to SPL, India stored in a freezer at −20 °C and analyzed immediately for various chemical components.

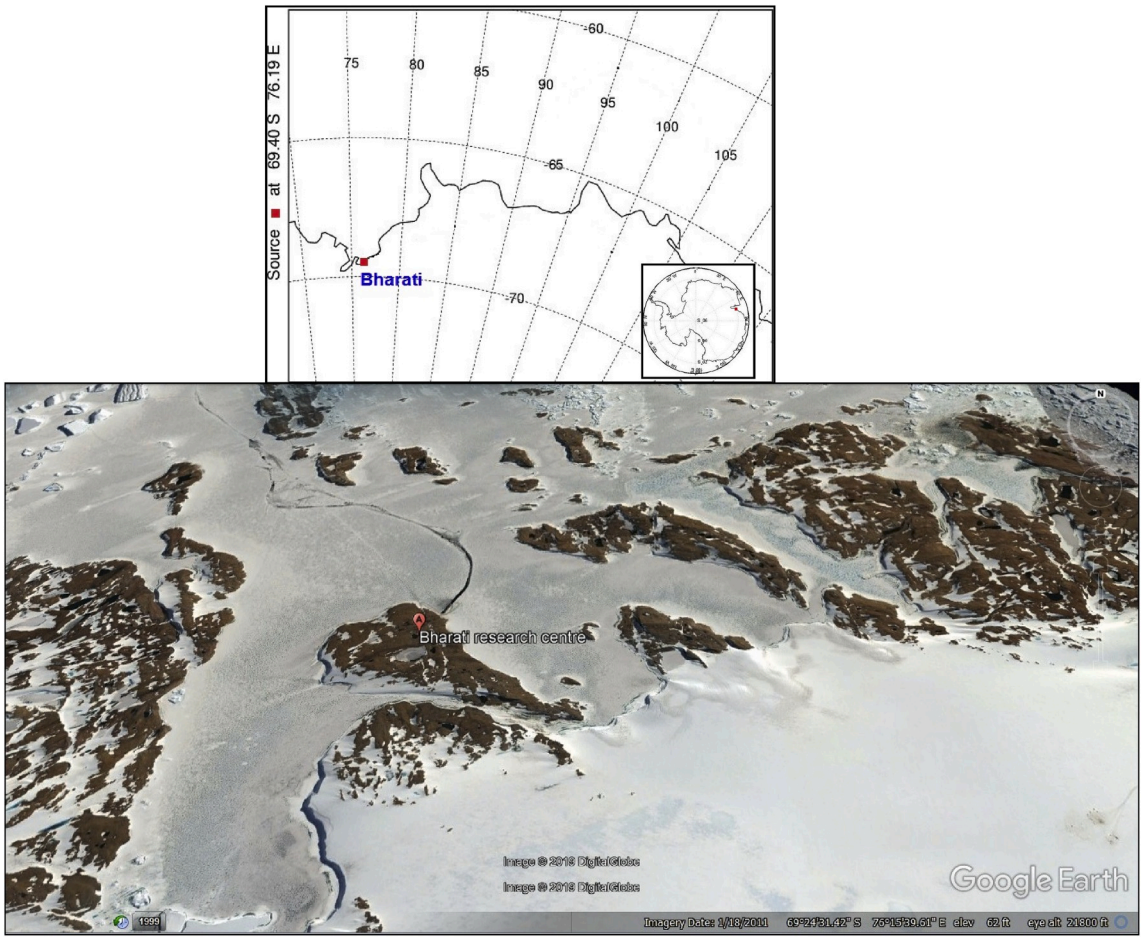

Fig. 1. Location of sampling site and its adjacent ice-free regions over the East Antarctic.

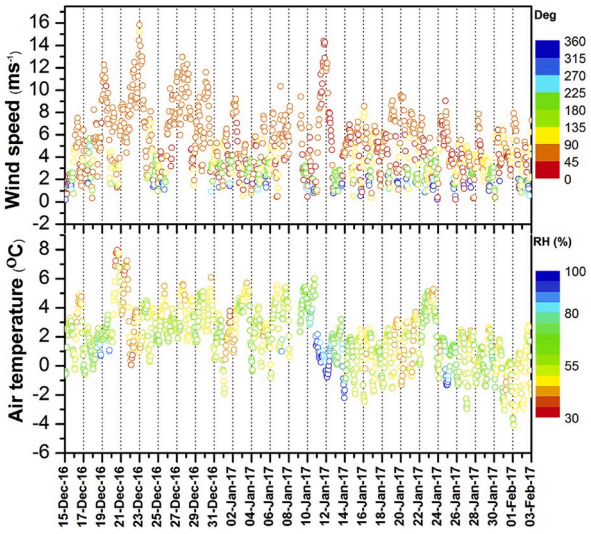

Fig. 2. Temporal variations of meteorological parameters (wind speed, wind direction, air temperature and relative humidity) during the study period that were collected at Indian meteorological station (IMD) near Bharati station.

The mass concentrations of PM_{10} samples (μg m^{-3}) were measured gravimetrically (difference between the initial and final weights of filters and the volume of air sampled). Filter samples were weighed thrice before and after the sampling using a digital microbalance (Satorius, model number LA 130 S–F) with a sensitivity of ±0.01 mg. Before weighing the aerosol samples, filters were almost dried by keeping in a desiccator at room temperature for about 24 h reducing the moisture in filter samples. Thick glass jars contain a silica gel crystal (a good absorber of moisture), which were initially heated to remove volatile contents present in it, were used as desiccators. Pre-baked (450 °C for 6h) glass bottles (250 ml) contain the filter samples were kept inside the desiccators for a while and the lid was closed properly so that the air cannot enter inside. This is a standard procedure and many researchers widely used in aerosol studies.

2.3. Chemical analyses

Carbonaceous species (organic carbon (OC) and elemental carbon (EC)) were determined using OC-EC analyzer (Sunset Laboratory Inc., USA) with a standard protocol of NIOSH-870 (National Institute of Occupational Safety and Health) (Chow et al., 2001) based on thermal-optical transmittance (TOT). An area (1.5 cm^2) of each filter was placed in a quartz boat inside the front oven and then stepwise heating was applied. Sucrose has been used to calibrate the OC-EC analysis and the recovery was >96%. The lower detection limit/sensitivity of the instrument is about 0.05 μg/sq cm.

Water-soluble organic carbon (WSOC) concentration was determined using a total organic carbon analyzer (TOC, Shimadzu, Japan). A known punch of filter sample was first extracted using organic-free ultra pure water (>18.2 MΩ resistivity, Sartorius arium 611 UV) followed by ultrasonication (30 min). These extracts were filtrated (Millex-GV, 0.22 mm pore size, Millipore) and injected into the TOC analyzer equipped with a catalytic oxidation column and non-dispersive infrared detector (NDIR). Calibration was performed with potassium nitrate. Water-

soluble total nitrogen (WSTN) was determined by decomposing the same sample in the combustion tube at 720°C, as result combustion products were converted nitrogen monoxide (NO) which is then detected by an ozone chemiluminescence detector. The concentrations of WSOC and WSTN in each sample were measured three times by the instrument and the deviation was less than 2% (Aswini et al., 2018).

To identify the water-soluble ionic species, a known amount of each filter was extracted with organic-free ultrapure water (resistivity of >18.2 MΩ, Sartorius arium 611 UV) followed by ultrasonicated (30 min) and then filtrated using disc filter (Millex-GV, 0.22 mm pore size, Millipore) to eliminate the insoluble matter and filter debris. These extracts were analyzed for major ions (MSA^-, Cl^-, SO_4^{2-}, NO_3^-, PO_4^{3-}, Na^+, NH_4^+, K^+, Ca^{2+}, and Mg^{2+}) using an ion chromatograph (882 Compact IC plus, Metrohm, Switzerland). A mixture of 3.2 mM Na_2CO_3 + 1 mM $NaHCO_3$ and 3 mM HNO_3 are used as eluents for anions and cations, respectively (Aswini et al., 2018).

The identification and quantification of metals (Fe, Al, Ca, Mg, Sr, Cr, Cu, Mo, Zn, Ni, Li, Co, Ti, V, Pb etc.) were performed using inductively coupled plasma-mass spectrometer (ICP-MS; Thermo Scientific, Model: iCAP Qc). In this method, an area of 6.28 cm^2 of each filter was placed into a Teflon digestion vessel and acidified with 5% of HNO_3, 2% of $HClO_4$ and 1% of HF. The acidified sample is digested in a microwave digester and extracted with 30 ml de-ionized water and filtrated using a disk filter (0.22 μm pore size, Satorius) and then bringing into the system.The sample is nebulised by the sample introduction system of ICP-MS into the core of inductively coupled argon plasma. In the presence of high temperature of the plasma, the nebulised sample is vaporized, and the sample species are atomized, and ionized subsequently. The generated ions are subsequently accelerated into a quadruple mass spectrometer that separates ions derived from a single mass-to-charge ratio (m/z). By comparison with the calibration standards (Multi element ICP standards, Reagecon), intensities are converted to elemental concentration at ppb levels.

2.4. Estimation of aerosol liquid water content

Aerosol liquid water content (ALWC) is a proxy for the aqueous-phase formation of atmospheric aerosols. It plays a huge role in the formation of secondary aerosol by enhancing the reaction rate of various chemical reactions can take place in the aqueous-phase atmosphere (Ervens et al., 2011; Seinfeld and Pandis, 2006). To understand the aqueous-phase formation of aerosols over the Antarctic, we estimated ALWC using an ISORROPIA II model (Fountoukis and Nenes, 2007). Chemical composition of aerosols and meteorological parameters (temp and RH) were used as input to this model and run on a reverse mode.

2.5. Quality assurance

To minimize the manual contamination, all possible precautions were taken meticulously during the collection and shipping of aerosol samples. To examine the analytical errors of the instruments used in this study, we performed triplicate analyses and results show that the errors were within 10%. Field blanks, obtained by loading filter to the sampler without starting the pump, collected during the sampling period and their contributions were ranged from 2 to 12% of real samples. Although some minor contaminations are detected for some chemical species (Ca^{2+} and Mg^{2+}), their concentration levels were lower than the blank levels. The reported concentrations for all measured chemical species and trace metals were suitably corrected against field blanks. We further checked the blank levels in ultra pure water and no peaks were observed in both anion and cation Chromatographs. Three and five point calibrations were performed using standards of known concentrations for all measured water-soluble species and elements. Non sea-salt concentrations of SO_4^{2-}, Ca^{2+} and Mg^{2+} were estimated using Na^+ as the sea-salt reference (Keene et al., 1986).

3. Results and discussions

3.1. PM_{10} mass

Total mass of PM_{10} at Bharati ranged from 2.4 to 16.3 μg m^{-3} (mean of 7.8 ± 3.3 μg m^{-3}) for the sampling period i.e., from December 17, 2016 to February 2, 2017. This mean value was higher than formerly reported value (5.1 ± 1.4 μg m^{-3}) for Bharati during summer 2009–10 (Budhavant et al., 2015) and James Rose island (6.4 ± 1.4 μg m^{-3} (Kavan et al., 2018),) but they were lower than those (8.2 ± 2.9 μg m^{-3}) reported for Maitri station (Chaubey et al., 2011; Gadhavi and Jayaraman, 2004); however, it was comparable to those reported for Norway sites (7.5 μg m^{-3}) (Pataud, 2010). In this study, the mean value of PM_{10} aerosols was also higher than those reported for McMurdo station for 1995–1997 (range: 3.5–4.2 μg m^{-3} (Mazzera et al., 2001),), the Antarctic Peninsula (Artaxo and Rabello, 1992), Marambio station during 2013–2015 (Asmi et al., 2018) and from Sevettijarvi site in Finland (annual mean: 4.4 μg m^{-3} (Pataud, 2010),). All these comparison studies may demonstrate that aerosols over Antarctica may be influenced by the various sources for example, different meteorological parameters, local source characteristics, changes in air mass origins, marine emissions etc., which will be discussed in the following sections, particularly over EA.

We found a clear temporal trend in PM_{10} mass concentrations at Bharati station, exhibiting lower values during 17 December to 8 January and higher during 9 January to 02 February (Fig. 3a). The highest concentration was observed on 9 Jan and lowest concentration

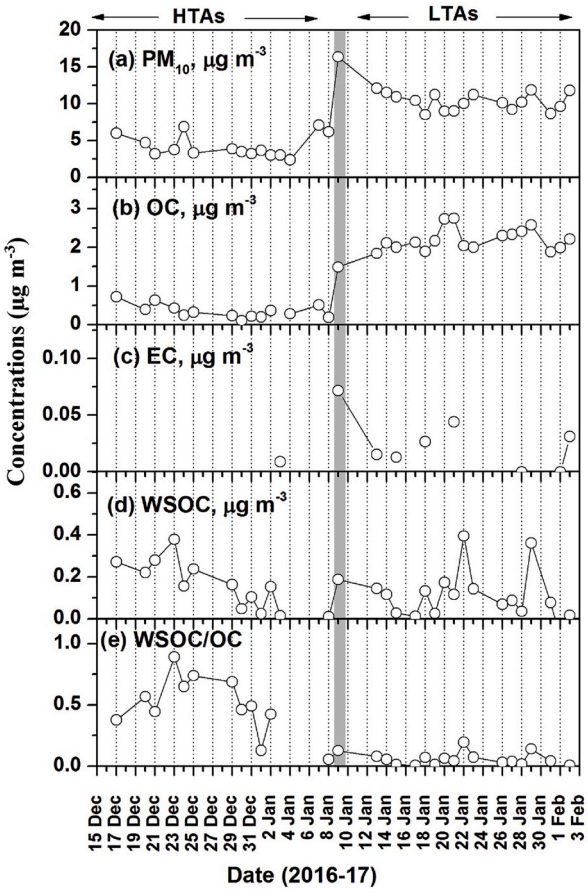

Fig. 3. Temporal variations of (a) Total PM_{10} mass, (b–d) carbonaceous aerosols, and (e) WSOC/OC mass ratios at Bharati station during summer of 2016–17. The shaded line divides the whole sampling period into two parts such as high altitude tropospheric aerosols (HTAs) and low altitude tropospheric aerosols (LTAs) aerosols.

was observed on 4 Jan. The observed highest concentration on 9 Jan was mainly associated with local anthropogenic activities those occurred in the vicinity of sampling site as personally reported in the log-book. An opposite trend was observed between PM_{10} mass and air temperature (Fig. 2), indicating a feasible link between the aerosol mass and local meteorology at Bharati. Based on the temporal variations observed in PM_{10} mass, meteorological parameters, air mass trajectories, and WSOC/OC ratios (will be discussed in the following section); we divided the whole sampling period into two regimes, i.e., 17 December to 8 January and 10 January to 02 February to better examine the characterization of aerosols and their short-term changes over the EA. It should be noted that we excluded the data point of Jan 9 in both regimes owing to the contamination by anthropogenic activities as aforementioned.

3.2. Characteristics of air masses and meteorological parameters

To better evaluate the impact of heterogeneity in air masses and their altitudinal variations on PM_{10} mass over the Antarctic, the 5-day air mass back trajectories were calculated using the HYSPLIT model (Draxler and Rolph, 2013) at an altitude of 200 m above the ground level of Bharati. The mean trajectories and their altitudinal variation with regard to time for both the periods are shown in Fig. 4a and b and d-e, respectively. We found an obvious difference in not only the origins of air masses, but also in their altitudes between the two periods. During the period i.e., from 17 December to 8 January, the air masses are coming from higher troposphere (means dominant air masses are coming from above the mixed layer height which will be discussed below) and stay longer time at high altitudes (>1000 m) prior to arriving at the sampling site and are considered as high-altitude-tropospheric air masses (HTAs), whereas in the later half (10 January to 02 February), the air mass transport pathways are very close to surface before reaching at the sampling site and thus deemed as low-altitude tropospheric air masses (LTAs). It is also noted that the sampling site is near to Open Ocean as aforementioned (Fig. 1 or Figure S1) thus; we should not ignore the influence of marine emissions (especially secondary formation) in addition to air mass transport.

Mixed layer depth (MLD), also known as mixed layer height, is the lowest region of the atmosphere, and is directly influenced by its proximity to the Earth's surface (Stull, 1988). Therefore, it is very useful to distinguish the aerosols are associated with either pristine (not mixed with pollutants) or polluted air masses (well mixed with pollutants in the atmosphere). Since MLD is a proxy for boundary layer height in the atmosphere, we downloaded MLD data from the website (http://www.arl.noaa.gov/HYSPLIT.php) for both the periods and is shown in Fig. 4c and f, respectively. In both periods, MLD showed a clear and systematic diurnal variation with higher values during noon hours (11:00 to 14:00) and lower values in night hours (see Fig. 4c, and f) as consistent with solar radiation. It is worthy to note that there was a significant difference ($p < 0.05$) in daytime MLD values between the two periods. The higher MLD values in HTAs may be owing to the higher solar radiations that were observed in HTAs (Fig. 2) and vice-versa. Mean MLD values varied between 240 and 700 m in HTAs while it was 91 and 500 m in LTAs. From Fig. 4a and b, it is obvious that MLD values were much below the mean height of air mass trajectories in HTAs, indicating that the air masses arriving from the above the mixed layer during their transport to sampling site (Fig. 4d). However, this is not the case in LTAs those were well mixed with pollutants within the boundary layer near the earth's surface (Fig. 4e). These inferences further confirm the influence pristine air masses during HTAs, while air masses are well mixed with near-surface pollutants (e.g., soil dust) in the LTAs over the sampling site. Therefore, we try to distinguish these changes in air masses (origin and height) in terms of chemical characterization and trace metals over the Antarctic as follows.

3.3. Differences in chemical characteristics of HTA and LTA aerosols

Table 1 summarizes the statistical report of measured and estimated mass concentrations of various chemical species and some of their specific ratios in PM_{10} aerosols for the two different periods over the Antarctic. Statistical analysis was performed using the *t*-test and results were reported in Table 1. A significant ($p < 0.05$) difference in PM_{10} mass concentrations was observed between the two periods and their

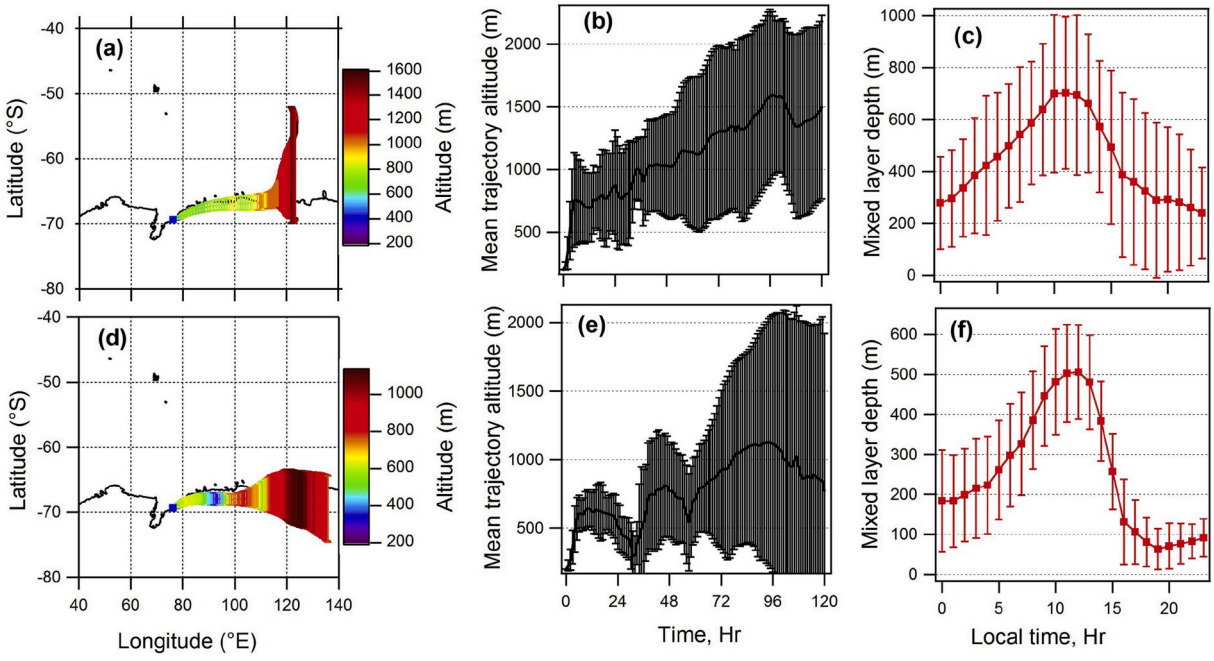

Fig. 4. Differences between the 120 h air mass back trajectories, mean trajectory altitudes (m), and mean diurnal variation of mixed layer depth for both the periods during the sampling period. Color scale indicates the mean altitudes of the trajectories (same as shown in d, e). Vertical lines passing through the lines are 1σ standard deviation. The upper panel (a, b, c) belongs to the high-altitude tropospheric aerosols (HTAs; Dec 17- Jan 8) whereas lower panel denotes low-altitude tropospheric aerosols (LTAs; Jan 8- Feb 2). (For interpretation of the references to color in this figure legend, the reader is referred to the Web version of this article.)

Table 1
Differences in the mass concentrations of identified chemical species (μg m^{-3}), specific mass ratios and trace elements (ng m^{-3}) in PM_{10} aerosols along with meteorological parameters between the high-altitude tropospheric aerosol (HTAs) and low-altitude tropospheric aerosols (LTAs) collected at Bharati, the coastal Antarctic station, during summer of 2017. We also performed statistical analysis in order to see the significant difference ($p < 0.05$, confidence level at 95%) between two different periods.

Chemical species	HTAs (Dec 17, 2016–Jan 8, 2017) (n = 15)			LTAs (Jan 10, 2017–Feb 02, 2017) (n = 17)			Statistical analysis		
	Min	Max	Mean ± SD	Min	Max	Mean ± SD	*t*-score	*df*	*p* value
PM_{10}	2.39	7.10	4.19 ± 1.42	12.1	8.53	10.3 ± 1.18	13	30	$p < 0.05$
OM	0.20	1.37	0.64 ± 0.33	3.50	5.22	4.18 ± 5.04	22	30	$p < 0.05$
EC	–	–	–	0.01	0.04	0.03 ± 0.01	–	–	–
WSOC	0.01	0.38	0.15 ± 0.12	0.01	0.39	0.12 ± 0.11	1.2	28	$p > 0.05$
WSTN	0.01	0.21	0.08 ± 0.06	0.01	0.36	0.12 ± 0.11	1.1	30	$p > 0.05$
MSA^-	0.02	0.12	0.04 ± 0.03	0.01	0.09	0.03 ± 0.02	0.7	28	$p > 0.05$
nss-SO_4^{2-}	0.19	0.53	0.27 ± 0.08	0.02	0.79	0.31 ± 0.15	0.9	30	$p > 0.05$
Cl^-	0.01	0.09	0.04 ± 0.03	0.06	0.28	0.12 ± 0.06	4.4	30	$p < 0.05$
PO_4^{3-}	0.01	0.75	0.12 ± 0.18	0.01	0.18	0.08 ± 0.06	0.9	30	$p > 0.05$
Na^+	0.12	0.22	0.16 ± 0.04	0.03	0.70	0.21 ± 0.16	1.1	30	$p < 0.05$
nss-Ca^{2+}	0.01	1.26	0.57 ± 0.30	0.01	2.26	1.16 ± 0.65	3.2	30	$p < 0.05$
Mg^{2+}	0.05	0.40	0.15 ± 0.08	0.02	0.42	0.19 ± 0.12	1.2	30	$p > 0.05$
Cl^-/Na^+	0.03	0.63	0.26 ± 0.18	0.09	2.59	0.87 ± 0.61	3.7	30	$p < 0.05$
WSOC/OC	0.05	0.89	0.49 ± 0.24	0.01	0.19	0.05 ± 0.05	7.4	27	$p < 0.05$
WSOM/WIOM	0.06	7.98	1.57 ± 2.10	0.01	0.24	0.06 ± 0.07	2.9	27	$p < 0.05$
Σ^+/Σ^-	2.48	7.27	4.34 ± 1.33	3.32	16.9	6.53 ± 3.24	2.4	31	$p < 0.05$
Ti, Titanium	1.02	14.3	10.3 ± 7.18	46.4	94.3	68.9 ± 16.7	10.3	26	$P < 0.05$
V, Vanadium	0.02	0.81	0.14 ± 0.21	0.19	0.89	0.46 ± 0.23	3.9	26	$p < 0.05$
Cr, Chromium	bdl	5.57	0.89 ± 1.77	bdl	10.1	2.22 ± 5.24	0.9	26	$p > 0.05$
Mn, Manganese	0.46	3.36	1.44 ± 1.66	0.27	1.93	1.09 ± 1.27	0.4	11	$p > 0.05$
Fe, Iron	57.6	397	177 ± 117	220	551	415 ± 148	4.7	26	$p < 0.05$
Co, Cobalt	bdl	0.17	0.09 ± 0.06	0.26	0.77	0.43 ± 0.13	7.4	21	$p < 0.05$
Ni, Nickel	–	–	–	0.14	15.3	4.96 ± 7.16	–	–	–
Cu, Copper	0.55	5.19	2.32 ± 1.51	3.10	22.5	8.09 ± 5.08	3.3	21	$p < 0.05$
Zn, Zinc	2.20	4.33	3.36 ± 1.50	0.73	31.9	9.92 ± 11.4	0.9	7	$p > 0.05$
As, Arsenic	bdl	0.16	0.05 ± 0.05	0.01	0.19	0.08 ± 0.08	0.9	19	$p > 0.05$
Se, Selenium	0.74	1.75	1.09 ± 0.57	0.06	2.35	1.35 ± 1.28	0.3	7	$p > 0.05$
Sr, Strontium	0.83	9.82	3.49 ± 4.28	0.34	2.66	1.69 ± 2.50	1.0	13	$p > 0.05$
Mo, Molybdenum	0.14	1.81	0.69 ± 0.47	0.03	0.25	0.17 ± 0.15	3.2	21	$p > 0.05$
Sb, Antimony	0.01	0.07	0.03 ± 0.02	0.04	0.38	0.18 ± 0.10	5.1	23	$p < 0.05$
Ba, Barium	4.26	16.9	11.5 ± 6.72	53.0	108	72.3 ± 15.9	13.1	23	$P < 0.05$
Pb, Lead	0.30	3.61	2.34 ± 1.48	7.52	23.5	13.1 ± 3.92	9.3	27	$p < 0.05$
Wind speed (ms^{-1})	0.34	15.8	5.64 ± 3.09	0.20	14.5	4.48 ± 2.56	2.0	31	$p > 0.05$
Temp (°C)	−1.8	7.98	3.01 ± 1.69	−4.09	6.00	1.02 ± 1.90	4.8	31	$p < 0.05$
RH (%)	36.0	90	53.5 ± 8.85	39.7	96.8	59.5 ± 13.4	1.3	31	$p > 0.05$

abundances were two times higher in LTAs than compared to HTAs. The composition of aerosols at Bharati was characterized by a high abundance of organic matter, calculated from the relation OM=OC*1.9 as suggested by previous studies (Simon et al., 2011; Turpin and Lim, 2001), followed by nss-Ca^{2+} and nss-SO_4^{2-} particles. Mass fractions of water-soluble inorganic matter (WSIM) were abundant (range: 19–70%) in HTAs while OM (and also WIOM) showed significant higher fractions (range: 30–60%) in LTAs, implying the abundance of secondary and primary emissions, respectively.

3.3.1. *Carbonaceous aerosols*

Temporal variations in the mass concentrations of carbonaceous aerosols including WSOC are shown in Fig. 3b–d. Consistent with PM_{10} mass, OM showed significant ($p < 0.05$) higher concentrations in LTAs, whose abundances were about eight times higher than compared to HTAs, whereas EC concentrations (a proxy for fossil fuel combustion aerosols) detected only in LTAs and their atmospheric abundances were very minor (0.01–0.04 μg m^{-3}) and were attributed to the so called in-situ emissions near the research stations. EC may be a good marker for biomass burning emissions through atmospheric long-range transport in remote regions, however, this is not appropriate at Bharati because there are several other research stations (for example, Zhongshan, Progress, Law base), existed in east or northeast directions within 2.5 km radius from each other, where the majority of LTAs are coming to the sampling site as shown in Figure S1. Therefore, it is reasonable to believe that the observed EC at Bharati may be due the combustion-derived aerosols arose from power generator filled with fuel near the other research stations although the position of the sampler was existed in upwind region at Bharati. On the other hand, WSOC showed slightly higher concentrations in HTAs (mean: 0.15 ± 0.12 μg m^{-3}) than those of LTAs (0.12 ± 0.11 μg m^{-3}). This slight enhancement of WSOC may suggest that importance of secondary formation of organic aerosols via atmospheric processing. On the other side, WSTN ranged from 0.01 to 0.36 μg m^{-3} (mean: 0.10 ± 0.08 μg m^{-3}) with higher concentrations ($p > 0.05$) during LTAs and lowered in HTAs (Table 1).

The water-soluble fraction of organic carbon (WSOC/OC) exhibited significant ($p < 0.05$) increase in HTAs (Fig. 3e) with about ten times higher than those of LTAs (Table 1). This inference suggests that aerosols in HTAs are photochemically processed and chemically aged in the atmosphere during their transport. Chemical aging traditionally increases the number of functional/oxidation groups and thus water solubility of organic aerosols in the atmosphere during their long-range transport (Boreddy et al., 2018; Kondo et al., 2007; Ram and Sarin, 2010). In contrast, lower WSOC/OC ratios of LTAs (Fig. 3e) are attributed to the primary emissions, which may be connected with rock or dust soil and combustion particles those finally deposited on the surface of snow/ice over the Antarctic. However, it is true that the decreasing trend of WSOC/OC ratios driven only increasing trend of OC (Fig. 3). In this view, we further investigated the primary and secondary sources of aerosols over the sampling site. Ceburnis et al. (2008) demonstrated that water-soluble organic matter (WSOM, [WSOC*1.9]) exhibited a downward flux, whereas water-insoluble organic matter (WIOM) exhibited an upward flux, thus it has been suggested that primary production for WIOM and a secondary formation associated with WSOM In this study, WSOM/WIOM ratios were ranged 0.06–7.98 (mean: 1.57 ± 2.10) in HTAs while 0.01–0.24 (0.06 ± 0.07) in LTAs (Table 1). The mean

WSOM/WIOM ratio in HTAs was about twenty five times higher to the LTAs indicating the dominance of secondary and primary emissions, respectively. This point further supports above inference that the secondary formation of water-soluble organic particles in HTAs and primary emissions associated with dust and other insoluble particles which are emitted from the other research stations (*in-situ* sources) which are existed in the pathways of LTAs as discussed above (Figure S1).

In fact, the majority of the ice will melt due to enhanced temperature (Fig. 2) as a result; ice-free regions may form in summer. These ice-free regions contain many insoluble particles for instance, EC and dust, which were deposited in the ice or snow, left on the rock surfaces will be blown into atmosphere by local winds. From Fig. 4e, it is clear that the air masses were initially originated at higher altitudes, build up a specific range of ripples or small scale mound during their transport and carry all these insoluble particles from the ice-free surfaces to the sampling site (Fig. 4d–f). In addition, summer time low moisture on surface and higher winds (overall mean ~5 ms^{-1}) make favor to uplift these soil/dust particles into the atmosphere (Wiggs et al., 2004).

3.3.2. *Water-soluble ionic species*

Except MSA^-, nss-SO_4^{2-}, Na^+ and phosphate (PO_4^{3-}), all compounds showed clear temporal variations with higher concentrations in LTAs and lowered in HTAs (Table 1). Cl^- concentrations were found to be vary between 0.01 and 0.28 μg m^{-3} during the whole study period and showed a clear temporal trend with significant higher values (mean: 0.12 ± 0.06 μg m^{-3}) in LTAs and lower values (0.04 ± 0.03 μg m^{-3}) in HTAs, while Na^+ concentrations did not show any temporal trend (range: 0.03–0.70 μg m^{-3}) as shown in Fig. 5 a-b. Chloride depletion, was estimated using the mass ratios of Cl^- to Na^+ ratios in sea water (1.8), ranged between 0.03 and 2.59 with an average of 0.59 ± 0.54, implying a significant chloride depletion over the sampling site and it was approximately four times higher in HTAs than those of LTAs (Table 1). This point further indicates the abundance of chemical reactions that occur during the chemical ageing in HTAs. PO_4^{3-} ranged from 0.01 to 0.75 μg m^{-3} with a mean of 0.10 ± 0.12 μg m^{-3}; however, it didn't show any significant variation between the two periods.

MSA^-, a photo oxidation product of DMS and also a proxy for biogenic emissions. It ranges between 0.01 and 0.12 μg m^{-3}. Consistent with WSOC variation, MSA^- showed higher values in HTAs than those of LTAs, though their difference was not significant ($p > 0.05$, Fig. 5c). Sulfate (SO_4^{2-}) particles primarily consist of non sea-salt (nss) SO_4^{2-} (>96%) which formed via gas to particle conversion of sulfur-bearing gases (for example, DMS). Concentrations of nss-SO_4^{2-} varied from 0.02 to 0.79 μg m^{-3} with higher values during LTAs and lower values in HTAs (Fig. 5d). A significant positive correlations ($p < 0.05$) were observed between the concentrations of MSA^- and nss-SO_4^{2-} in both the periods (Fig. 6a) and the correlation coefficient (R^2) was significantly ($p < 0.05$) higher ($R^2 = 0.78$) in HTAs than compared to LTAs ($R^2 = 0.33$). These inferences suggest that both MSA^- and nss-SO_4^{2-} were formed from a single source, i.e., photo-oxidation of DMS and/or heterogeneous oxidation of SO_2 in the aqueous-phase atmosphere and this process was more abundant in HTAs. Since MSA comes only from the oxidation of DMS, the relative mass contribution of MSA^- to nss-SO_4^{2-} can be used as an indicator of marine or continental influences (Gondwe et al., 2004; Legrand and Pasteur, 1998; Savoie and Prospero, 1989). Higher ratios indicate the atmospheric oxidation of oceanic DMS, while lower ratios attributed to the continental emissions. The median (mean) MSA^-/nss-SO_4^{2-} ratios were 0.12 (0.12 ± 0.05) and 0.08 (0.13 ± 0.21) in HTAs and LTAs, respectively. This result suggests that substantial contribution of marine biogenic DMS oxidations in HTAs while non marine sources, such as the anthropogenic activities in the vicinity of research stations or resuspension of the soil as primary particles, in LTAs. These mean values at Bharati were higher than those reported for PM_{10} aerosols (0.02) at the Marambio station in the Antarctic Peninsula

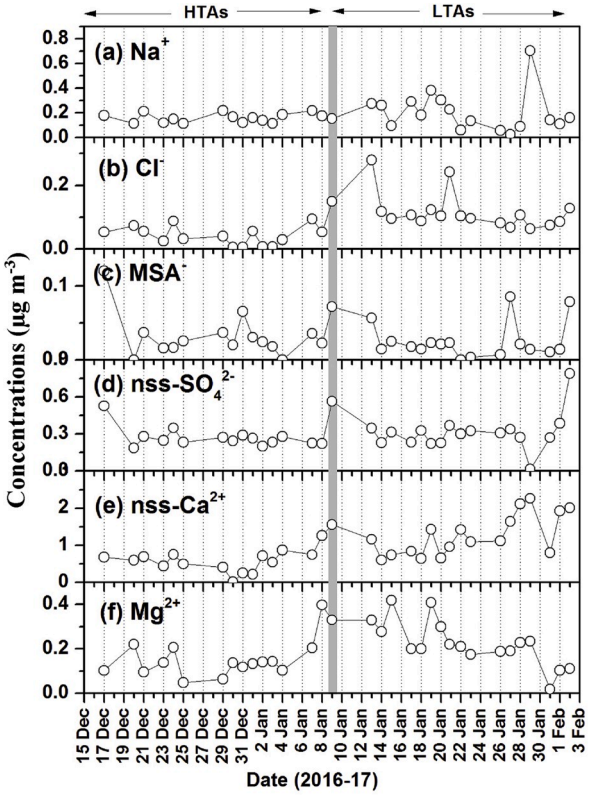

Fig. 5. Temporal variations of water-soluble ionic species (μg m^{-3}) in PM_{10} aerosols at Bharati, East Antarctica. The shaded line divides the whole sampling period into two parts such as high altitude tropospheric aerosols (HTAs) and low altitude tropospheric aerosols (LTAs) aerosols.

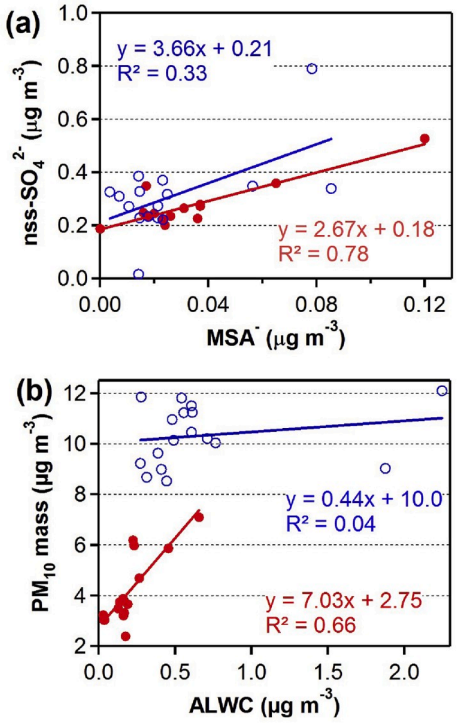

Fig. 6. Regression analysis, (a) MSA^- vs. nss-SO_4^{2-} and (b) ALWC vs. PM_{10} mass during the sampling period at Bharati. Red and blue colors indicate aerosols associated with HTAs and LTAs, respectively. (For interpretation of the references to color in this figure legend, the reader is referred to the Web version of this article.)

(Asmi et al., 2018). Further Weller and Wagenbach (2007) documented that MSA^-/nss-SO_4^{2-} ratios which reached at Kohnen its maximum of 0.33 during fall while at Neumayer a maximum value of 0.36 appeared in summer. Similarly, at the coastal Antarctic site, Kohnen, the mean MSA^-/nss-SO_4^{2-} values under clear sky conditions were 0.18 ± 0.03 and 0.22 ± 0.13 during the summer campaigns in 2015 and 2016, respectively (Weller et al., 2018).

To further examine the formation of PM_{10} aerosols at Bharati, We estimated ALWC values using the ISORROPIA-II model as discussed in Section 2.1. ALWC showed a significant ($p < 0.05$) correlation ($R^2 = 0.67$) with PM_{10} mass in HTAs while there is no such correlation was observed in LTAs (Fig. 6b). Along with high WSOC/OC as well as WSOM/WIOM ratios and high temperature (see Table 1 and Figs. 2b, and Fig. 3d), this inference suggests that the aqueous-phase formation may be the significant pathway of aerosols in HTAs. In fact, it is well known that aerosol water content usually enhances the reaction rate of formation of water-soluble portion of aerosols or secondary aerosols thus it has been suggested as a proxy for the aqueous-phase formation of aerosols. However, it does not explain the water-insoluble portion of aerosols, such as dust and other primary aerosols. The fraction of water-soluble matter (WSM) to PM_{10} mass was higher (37%) in HTAs and lower in (22%) in LTAs and vice-versa. This point further supports the aqueous-phase formation of aerosols in HTAs.

nss-Ca^{2+}, a proxy for dust aerosols, was the most abundant among all water-soluble ionic species determined in PM_{10} aerosols and showed significantly ($p < 0.05$) higher concentrations in LTAs and their atmospheric abundance were twice to those of HTAs (Fig. 5e, and Table 1), suggesting that the dominance of dust emissions in the EA, especially in LTAs as discussed in section 3.1. Similarly, Mg^{2+} showed higher concentrations in LTAs, despite their difference in two periods were not significant ($p > 0.05$). It was further found that a significant positive correlation ($y = 2.1x+0.2$; $R^2 = 0.35$; $p < 0.05$) exists between Mg^{2+} and nss-Ca^{2+}, implying that both are coming from similar sources, perhaps soil/dust emissions. Traditionally, Mg^{2+} should correlate with Na^+ over the marine environment; however, we did not find any correlation between them at Bharati during both HTAs and LTAs as shown in Figure S2. Mg^{2+}/Na^+ mass ratios were ranged 0.29–2.27 (0.98 ± 0.55) and 0.12–6.41 (1.70 ± 1.73) in HTAs and LTAs, respectively. These mean values are very far away from the seawater ratio of Mg/Na i.e., 0.012 (Chesselet et al., 1972), suggesting an additional source of Mg^{2+} other than sea-salts over the sampling site. Further, the contribution of nss-Mg^{2+} was about >98% to total Mg^{2+} mass concentration. Both nss-Ca^{2+} and nss-Mg^{2+} showed significant ($p < 0.05$) higher concentrations in LTAs compared to HTAs. All these results suggest that the major contribution of non-sea-salt sources to Mg^{2+} at Bharati during the sampling period.

Molar equivalent ratio (Σ^+/Σ^-), a proxy for aerosol acidity, defined as the ratio of total molar equivalents of cations to the anions (excluding the hydronium ion, H^+), with lower ratios (less than unity) correspond to particles with the acidity and higher ratios (>unity) may be indicated alkaline aerosols. The Σ^+/Σ^- ratios were ranged 2.48–7.27 (4.34 ± 1.33) and 3.32–16.9 (6.53 ± 3.24) in HTAs and LTAs, respectively (Table 1), suggesting the alkaline nature of aerosols. Generally, in Antarctica, in summer, the anion content should be higher due to the presence of high concentration of SO_4^{2-} and NO_3^-, however, no such a case observed at Bhatati. In fact, high loading of mineral dust (Ca^{2+} and Mg^{2+}) may play a key role to make aerosol neutralize/alkaline at Bharati. Further, the Lower Σ^+/Σ^- ratios in HTAs were explained by the higher chloride loss via heterogeneous reactions as aforesaid. All these results demonstrated that the aerosols collected at Bharati have alkaline nature, thus significant implications toward climate change over the EA. It is noteworthy that size may also play an important role on nature of aerosols, therefore, size segregated aerosols may give different results.

We roughly estimated reconstructed PM_{10} mass using measured chemical species as well as estimated (CO_3^{2-}). Since higher concentrations of mineral dust were observed in PM_{10}, there may be significant contribution of carbonate (CO_3^{2-}) in aerosol particle at Bharati, thus we have estimated CO_3^{2-} [1.5nss-Ca^{2+}+2.5nss-Mg^{2+}] in PM_{10} aerosols based on the method described elsewhere (Querol et al., 2001; Malaguti et al., 2015). On average, the reconstructed PM_{10} mass [all measured inorganic ions + CO_3^{2-} + OM + Trace metals] were 86% and 93% of the measured PM_{10} mass in HTAs and LTAs, respectively. The rest may be the error in mass determination by weight.

3.3.3. Trace metals

The trace metals Ti, V, Cr, Mn, Fe, Co, Ni, Cu, Zn, As, Se, Sr, Mo, Cd, Sn, Sb, Ba, and Pb were identified in PM_{10} aerosols at Bharati to get a better understanding of natural geochemical variability of soils present over EA because soils are persistent indicators of environmental change and human impacts. Among all identified trace metals, Fe and Ba are most abundant in both the air masses. The elemental distribution was characterized Fe > Ba > Ti > Sr > Zn in HTAs while it was Fe > Ba > Ti > Pb > Zn in LTAs. The mean total trace metal concentration was more than a couple of times higher in LTAs (639 ± 171 ng m^{-3}) than those of HTAs (250 ± 145 ng m^{-3}). Temporal variations of selected typical trace metals are shown in Fig. 7a–g. Fe and Ti are the typical tracers of crustal elements produced in the atmosphere by mechanical erosion of soil/dust (Nriagu and Pacyna, 1988). Concentrations of Fe were varied from 57 to 396 ng m^{-3} (177 ± 117 ng m^{-3}) and 220–550 ng m^{-3} (415 ± 148 ng m^{-3}) in HTAs and LTAs, respectively. Their atmospheric abundances were more than two times higher in HTAs than those of LTAs. The abundance of Ti was more than six times higher in LTAs (range: 46.4–94.3 ng m^{-3}; mean: 68.9 ± 16.7 ng m^{-3}) than those of HTAs (1.02–14.3 ng m^{-3}; 10.3 ± 7.18 ng m^{-3}). Similarly Co also associated with soil/dust emissions showed higher concentrations in LTAs (0.43 ±

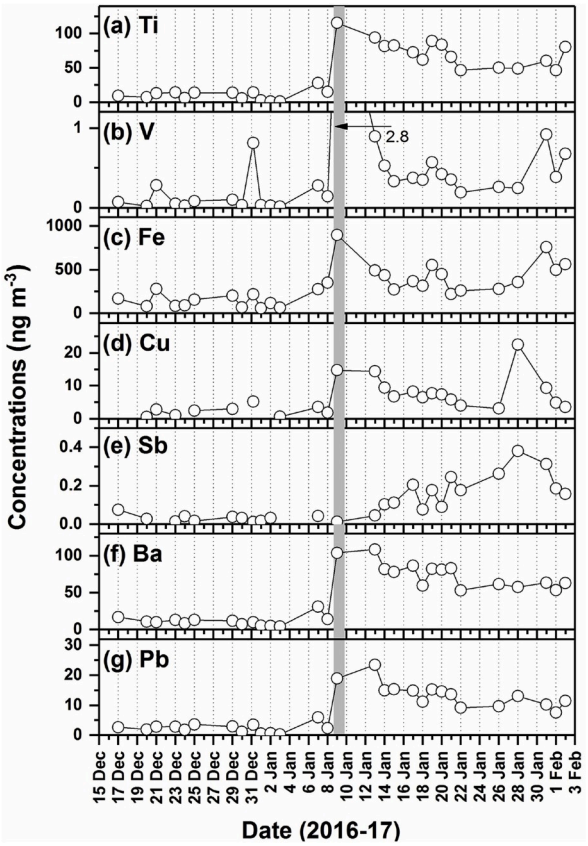

Fig. 7. Temporal variations of major trace metal species in PM_{10} aerosols at Bharati.
The shaded line divides the whole sampling period into two parts such as high altitudeTropospheric
aerosols (HTAs) and low altitude tropospheric aerosols (LTAs) aerosols.

0.13 ng m^{-3}) and their abundance was four times higher to the HTAs (0.09 ± 0.06 ng m^{-3}). On the other hand, it has also been documented that combustion processes are vital sources of anthropogenic aerosol fraction of trace metals such as Pb, Zn, Cu, As, Sb, V (Nriagu, 1979, 1989). The mean concentrations of V, Cu, Sb, Pb, and Zn, were 0.14 ± 0.21 ng m^{-3} (0.46 ± 2.3 ng m^{-3}), 2.32 ± 1.51 ng m^{-3} (8.09 ± 5.08 ng m^{-3}), 0.02 ± 0.03 ng m^{-3} (0.18 ± 0.10 ng m^{-3}), 2.34 ± 1.48 ng m^{-3} (13.3 ± 3.92 ng m^{-3}), and 3.26 ± 1.50 ng m^{-3} (9.92 ± 11.4) in HTAs (LTAs), respectively. The atmospheric abundance of all these metals are several times higher in LTAs than those of HTAs at Bharati during the sampling period. Further, Ba is second most abundant metal is showed significant higher concentrations in LTAs and its abundance was six times higher compared to HTAs. Ba is likely comes from the incineration of electronic waste (Deng et al., 2006). All these inferences suggest that LTAs were perhaps dominated by natural crustal emissions as well as combustion-derived anthropogenic emissions (*in-situ* emissions). This point further supported by a significant ($p < 0.05$) correlation of Ti, Fe and Pb with PM_{10} mass in LTAs as shown in Figure S3. It is shown that higher correlation coefficients (R^2) were observed in LTAs than those of HTAs, again indicating the importance of soil-derived and in-situ emissions in LTAs. Enrichment factors were estimated using Fe as a reference metal [$EF=(Metal/Fe)_{aerosol}/(Metal/Fe)_{crust}$] and upper continental crust values taken from elsewhere (Wedepohl, 1995) (Fig. 8). EF values are close to unity suggest that trace metal concentration may come entirely from natural or physical weathering processes, otherwise it indicates that a significant portion of the trace metals was delivered from non-crustal materials (Barbieri, 2016). In this view, it is obvious that elements like Ni, Cu, Zn, Sb, and Pb showed high EFs (>10) can be considered to be from anthropogenic emissions. On the other hand, EFs of Ti, Mn and Sr are around 1, suggesting the crustal sources are major inputs to these metals. Pb exhibited higher EF values among reported elements in PM_{10} aerosols at Bharati.

Literature studies confirmed that huge amount of metals are emitted into the Antarctic atmosphere as result of human activities (Lu et al., 2012; Santos et al., 2005) near the research stations. These human-made activities significantly invade concentration levels of various elements in the Antarctic, and make it difficult to evaluate, whether the metals derive from natural or anthropogenic sources. To better understand the impact of research activities (so called in-situ sources) on soil trace metal contamination, Shi et al. (2018) collected Topsoils from LHs in the East Antarctica and analyzed for trace metals. They found elevated Pb levels inside the research stations compared to those outside the station areas and attributed it to the human anthropogenic activities. In this study, Pb concentrations were higher in LTAs (Fig. 7g) and their abundances were about six times higher compared to HTAs, implying the anthropogenic influences associated with human activities in LTAs over the EA.

It is further reported that sediments and/or soils' surface are the major reservoirs for trace metals in the Antarctica (Santos et al., 2005). Generally, soil development engages physical and chemical mineralogical changes in the Antarctic is inhibited by various processes including ion exchange, acid-base reactions, adsorption, and erosion of rocks etc., have an effect on the distribution of metals in soils (Potapowicz et al., 2019). In fact, due to lower temperatures, alkaline nature of aerosols and very sparse micro-organisms in LHs' soil (Hopkins et al., 2005; Signh et al., 2007), chemical weathering may not be possible sources of soil emissions at Bharati. Therefore, soils at LHs are probably caused by physical weathering (mechanical erosion) of local basement rocks, such as gneiss, granulite and granite (Carson et al., 1995; Gasparon and Matschullat, 2006; Shi et al., 2018). It is reasonable because in LHs, particularly in the surrounding areas of research stations, soils are severely disturbed by human activities, such as building or road constructions and vehicle grindings, as a result, wobbly soils widely distributed and are uplifted into the atmosphere by local winds. Therefore, the physical weathering process in ice-free surfaces may be a significant source of aerosols (high loading of dust) over the EA during summer. Based on these results, we suggest that soil-derived emissions and local anthropogenic emissions (*in-situ* emissions) are possible sources at Bharati, especially at LTAs.

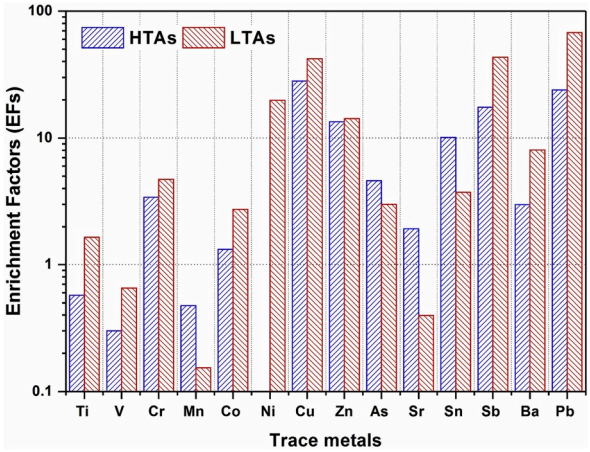

Fig. 8. Enrichment factors for each metal in PM_{10} aerosols during HTAs and LTAs at Bharati station in East Antarctica.

4. Summery and conclusions

The present study reports on carbonaceous aerosols, water-soluble species and trace metals in PM_{10} aerosols collected at Bharati in the East Antarctica during the period from December 17, 2016 to February 2, 2017. The results from this study provide the following findings.

1. Chemical composition at Bharati characterized by high abundance of organic matter followed by mineral dust particles (nss-Ca^{2+} and Mg^{2+}). A key finding is that significant differences in the mass concentrations of all measured species in PM_{10} aerosols were associated with air masses originated from HTAs clearly distinguishable those from LTAs as inferred from the Hysplit backward trajectory analysis.
2. Carbonaceous aerosols, water-soluble matter and dust particles showed higher concentrations in LTAs than those of HTAs.
3. Significant correlations between MSA^- and nss-SO_4^{2-} suggest that they have common source associated with DMS oxidation, particularly in HTAs. Moreover, WSOC/OC and WSOM/WIOM mass ratios suggest that photochemical oxidations of secondary organic aerosols and primary emission are major sources in HTAs and LTAs, respectively.
4. PM_{10} aerosols collected at Bharati showed alkaline nature due to erosion of soil/dust particles from the ice-free regions from vicinity of the sampling site.
5. The trace metal analysis revealed that high abundance of trace elements like Fe, Ti, Pb, Ba, and V in LTAs than those of HTAs further suggesting that soil-derived emissions and local anthropogenic sources (so called in-situ emissions) are possible sources of PM_{10} aerosols, especially when LTAs arrived at the sampling site. This point further supported by significant ($p < 0.05$) correlation of PM_{10} with Ti and Pb in LTAs as well as the enrichment factor analysis.

The present study demonstrated that ice-free regions in EA may be able to act as significant sources of aerosols by providing mineral dust as well as so called *in-situ* emissions which may play a major role in Antarctic climate by increasing the aerosol loading in Antarctic atmosphere. This study further suggests that more detailed and continuous investigations should be required to monitor the particulate matter and its sources for a better protection of the pristine environment of Antarctica.

Acknowledgements

This work has been done as part of 36th ISEA, conducted by the

National Centre for Antarctic and Ocean Research (NCAOR), Goa. The authors thank the Director, NCAOR and his team for arranging necessary logistics and support for conducting the sampling at Bharati. The authors greatly acknowledge NOAA Air Resources Laboratory for free access of the HYSPLIT transport dispersion model from the website, http://www.arl.noaa.gov/HYSPLIT.php. The authors thank Mr. Santosh Muralidharan for his help with aerosol sampling. The authors kindly acknowledge Dr. Prabha R Nair for her scientific discussion during the manuscript preparation. Dr. Boreddy is thankful to ISRO for his research fellowship. All the data presented in this paper are available up on a request to the corresponding author.

Appendix A. Supplementary data

Supplementary data to this article can be found online at https://doi.org/10.1016/j.polar.2020.100520.

References

Ali, K., Trivedi, D.K., Sahu, S., 2015. Physico-chemical characterization of total suspended particulate matter over two coastal stations of Antarctica and adjoining ocean. Atmos. Environ. 122, 531–540.

Artaxo, P., Rabello, M.L.C., 1992. Trace elements and individual particle analysis of atmospheric aerosols from the Antarctic Peninsula. Tellus B 44, 318–334.

Asmi, E., Neitola, K., Teinila, K., Rodriguez, E., Virkkula, A., Backman, J., al, e., 2018. Primary sources control the variability of aerosol optical properties in the Antarctic Peninsula. Tellus B 70, 1414571.

Aswini, A.R., Hegde, P., Nair, P.R., 2018. Carbonaceous and inorganic aerosols over a sub-urban site in peninsular India: temporal variability and source characteristics. Atmos. Res. 199, 40–53.

Ayers, G.P., Gras, J.L., 1991. Seasonal relationship between cloud condensation nuclei and aerosol methanesulfonate in marine air. Nature 353, 834–835.

Bao, H., Campbell, D.A., Bockheim, J.G., Thiemens, M.H., 2000. Origins of sulphate in Antarctic dry-valley soils as deduced from anomalous 17O compositions. Nature 407, 499–502.

Barbaro, E., Zangrando, R., Kirchgeorg, T., Bazzano, A., Illuminati, S., Annibaldi, A., Rella, S., Truzzi, C., Grotti, M., Ceccarini, A., Malitesta, C., Scarponi, G., Gambaro, A., 2016. Anintegrated study of the chemical composition ofAntarctic aerosol to investigate natural and anthropogenic sources. Environ. Chem. 13, 867–876.

Barbieri, M., 2016. The importance of enrichment factors (EF) and Geoacculation index (I_{geo}) to evaluate the soil contamination. J. Geol. Geophys. 5, 1. https://doi.org/10.4172/2381-8719.1000237.

Bargagli, R., Agnorelli, C., Borghini, F., Monaci, F., 2005. Enhanced deposition and bioaccumulation of mercury in antarctic terrestrial ecosystems facing a coastal polynya. Environ. Sci. Technol. 39, 8150–8155.

Bargagli, R., Monaci, F., Bucci, C., 2007. Environmental biogeochemistry of mercury in Antarctic ecosystems. Soil Biol. Biochem. 39, 352–360.

Boreddy, S.K.R., Haque, M.M., Kawamura, K., 2018. Long-term (2001-2012) trends of carbonaceous aerosols from remote island in the western North Pacific: an outflow region of Asian pollutants and dust. Atmos. Chem. Phys. 2018, 1291–1306.

Bory, A., Wolff, E., Mulvaney, R., Jagoutz, E., Wegner, A., Ruth, U.e.a., 2010. Multipul sources supply eolian mineral dust to the Atlantic sector of coastal Antarctica: evidence from the recent snow layers at the top of Berkner Island ice sheet. Earth Planet Sci. Lett. 291, 138–148.

Budhavant, K., Rao, P.S.P., Safai, P.D., 2016. Size distribution and chemical composition of summer aerosols over Southern Ocean and the Antarctic region. J. Atmos. Chem. 74, 491–503.

Budhavant, K., Safai, P.D., Rao, P.S.P., 2015. Sources and elemental composition of summer aerosols in the LArsemann Hills (Antarctica). Environ. Sci. Pollut. Res. 22, 2041–2050.

Bullard, J.E., Baddock, M., Bradwell, T., Crusius, J., Darlington, E., Gaiero, D.e.a., 2016. High-latitude dust in the earth system. Rev. Geophys. 54, 447–485.

Carson, C., Dirks, P., Hand, M., Sims, J., Wilson, C., 1995. Compressional and extensional tectonics in low-medium pressure granulites from the Larsemann Hills, East Antarctica. Goel. Mag. 132, 151–170.

Ceburnis, D., O'Dowd, C.D., Jennings, G.S., Facchini, M.C., Emblico, L., Decesari, S., Fuzzi, S., Sakalys, J., 2008. Marine aerosol chemistry gradients: elucidating primary and secondary processes and fluxes. Geophys. Res. Lett. 35, L07804 https://doi.org/10.1029/2008GL033462.

Chaubey, J.P., Moorthy, K.K., Babu, S.S., Nair, V.S., 2011. The optical and Physical properties of atmospheric aerosolsover the Indian Antarctic stations during southern hemispheric summer of the international Polar Year 2007-2008. Ann. Geophys. 29, 109–121.

Chesselet, R., Morelli, J., Buat-Menard, P., 1972. Variations in ionic ratios between reference sea-water and marine aerosols. J. Geophys. Res. 77, 5116–5131.

Deng, W.J., et al., 2006. Atmospheric levels and cytotoxicity of PAHs and heavy metals in TSP and $PM_{2.5}$ at an electronic waste recycling site in southeast China. Atmos. Environ. 40, 6945–6955.

Draxler, R.R., Rolph, G.D., 2013. HYSPLIT (HYbrid single–particle Lagrangian integrated trajectory) model, access via NOAA ARL READY website. available at: http://www.arl.noaa.gov/HYSPLIT.php.

Du, Z., Xiao, C., Ding, M., Li, C., 2018. Identification of multiple natural and anthropogenic sources of dust in snow from Zhongshan Station to Dome A, East Antarctica. J. Glaciol. 64, 855–865.

Ervens, B., Turpin, B.J., Weber, R.J., 2011. Secondary organic aerosol formation in cloud droplets and aqueous particles (aqSOA): a review of laboratory, field and model studies. Atmos. Chem. Phys. 11, 11069–11102.

Fountain, A.G., Nylen, T.H., Monaghan, A., Basagic, H.J., Bromwich, D., 2009. Snow in the McMurdo dry valleys, Antarctica. Int. J. Climatol. 30, 633–642.

Fountoukis, C., Nenes, A., 2007. Isorropia II: a computationally efficient thermodynamic equilibrium model for K+-Ca2+-Mg2+-Nh(4)(+)-Na+-SO42–NO3–Cl–H2O aerosols. Atmos. Chem. Phys. 7, 4639–4659.

Gadhavi, H., Jayaraman, A., 2004. Aerosol Characteristics and aerosol radiative forcing over Antarctica. Curr. Sci. 86 (2), 1–25.

Gasparon, M., Matschullat, J., 2006. Geogenic sources and sinks of trace metals in the Larsemann Hills, East Antarctica: natural processes and human impact. Appl. Geochem. 21, 318–334.

Giordano, M., Kalnajs, L., Avery, A., Goetz, J.D., Davis, S.M., DeCarlo, P.F., 2017. A missing source of aerosols in Antarctica – beyond long-range transport, phytoplankton, and photochemistry. Atmos. Chem. Phys. 17, 1–20.

Gondwe, M., Krol, M., Klaassen, W., Gieskes, W., de Baar, H., 2004. Comparison of modelled versus measured MSA: nss-SO_4^{2-} ratios: a Global analysis. Global Biogeochem. Cycles 18, GB2006. https://doi.org/10.1029/2003GB002144.

Gogoi, M.M., Babu, S.S., Pandey, S.K., Nair, V.S., Vaishya, A., Girach, I.A., Koushik, N., 2018. Scavenging ratio of black carbon in the Arctic and the Antarctic. Polar Sci. 16, 10–22.

Hara, K., Osada, K., Kido, M., Hayashi, M., Matsunaga, K., Iwasaka, Y., Yamanouchi, T., Hashida, G., Fukatsu, T., 2004. Chemistry of se-salt particles and inorganic halogen species in Antarctic regions: compositional differences between coastal and inland stations. J. Geophys. Res. 109, D20208.

Hodgson, D.A., Noon, P.E., Vyverman, W., Bryant, C.L., Gore, D.B., Appleby, P., Gilmour, M., Verleyen, E., Sabbe, K., Jones, V.J., Ellis-Evans, J.C., Wood, P.B., 2004. Were the Larsemann hills ice-free through the last glacial maximum? Antarct. Sci. 13, 440–454.

Hong, S., Lluberas, A., Lee, G., Park, J.K., 2002. Natural and anthropogenic heavy metal deposition to the snow in king george island. Antarct. Peninsula Ocean Polar Res. 24, 279–287.

Hopkins, D., Elberling, B., Greenfield, L., Gregorich, E., Novis, P., O'Donnell, A., Sparrow, A., 2005. Soil Micro-organisms in Antarctic Dry Valleys: Resource Supply and Utilization. In: Symposia-Scoiety for General Microbiology, 1999. Cambridge University Press, Cambridge, p. 71.

Jourdain, B., Legrand, M., 2002. Year-round records of bulk and size-segregated aerosol composition and HCl and HNO_3 levels in the Dumont d'Urville (coastal Antarctica) atmosphere: implications for sea-salt aerosol fractionation in the winter and summer. J. Geophys. Res.: Atmosphere 107. ACH 20-21-ACH 20-13.

Jung, J., Hong, S., Chen, M., Hur, J., Jiao, L., Lee, Y., Park, K., Hahm, D., Choi, J., Yang, E.J., Park, J., Kim, T., Lee, S., 2019. Characteristics of biogenically-derived aerosols over the amundsen sea, Antarctica. Atmos. Chem. Phys. Discuss. https://doi.org/10.5194/acp-2019-133.

Kavan, J., Dagsson-Waldhauserova, P., Renard, J.B., Laska, K., Ambrozova, K., 2018. Aerosol concentrations in relationship to local atmospheric conditions on James Ross Island, Antarctica. Front. Earth Sci. 6.

Kavan, J., Nyvlt, D., 2018. Blowing in the wind-where does the Antarctic fluvial suspended load come from ?. In: Proceedings of the Polar 2018-SCAR& IASC Conference, Davos.

Kawamura, K., Sempéré, R., Imai, Y., Fujii, Y., Hayashi, M., 1996. Water soluble dicarboxylic acids and related compounds in Antarctic aerosols. J. Geophys. Res. Atmos. 101, 18721–18728.

Keene, W.C., Pszenny, A.A.P., Galloway, J.N., Hawley, M.E., 1986. Sea-salt corrections and interpretation of constituent ratios in marine precipitation. J. Geophys. Res.: Atmosphere 91, 6647–6658.

Kerminen, V.-M., Teinilä, K., Hillamo, R., 2000. Chemistry of sea-salt particles in the summer Antarctic atmosphere. Atmos. Environ. 34, 2817–2825.

Kondo, Y., Miyazaki, Y., Takegawa, N., Miyakawa, T., Weber, R.J., Jimenez, J.L., Zhang, Q., Worsnop, D.R., 2007. Oxygenated and water-soluble organic aerosols in Tokyo. J. Geophys. Res. Atmos. 112.

Kreidenweis, S.M., Seinfeld, J.H., 1988. Nucleation of sulfuric acid-water and methanesulfonic acid-water solution particles: implications for the atmospheric chemistry of organosulfur species. Atmos. Environ. 22, 283–296.

Legrand, M., Pasteur, E.C., 1998. Methane sulfonic acid to non seasalt sulfate ratio in coastal Antarctic aerosol and surface snow. J. Geophys. Res. 103 (D9), 10991–11006.

Legrand, M., Preunkert, S., Wolff, E., Weller, R., Jourdain, B., Wagenbach, D., 2017. Year-round records of bulk and size-segregated aerosol composition in central Antarctica (Concordia site) – Part 1: fractionation of sea-salt particles. Atmos. Chem. Phys. 17, 14039–14054.

Legrand, M., Sciare, J., Jourdain, B., Genthon, C., 2001. Subdaily variations of atmospheric dimethylsulfide, dimethylsulfoxide, methanesulfonate, and non-seasalt sulfate aerosols in the atmospheric boundary layer at Dumont d'Urville (coastal Antarctica) during summer. J. Geophys. Res. 106 (D13), 14409–14422.

Lim, S., Lee, M., Rhee, T.S., 2019. Chemical characteristics of submicron aerosols observed at the King Sejong Station in the northern Antarctic Peninsula from fall to spring. Sci. Total Environ. 668, 1310–1316.

Liu, J., Dedrick, J., Russell, L.M., Senum, G.I., Uin, J., Kaung, C., Springston, S.R., Leaitch, W.R., Aiken, A.C., Lubin, D., 2018. High summertime aerosol organic functional group concentrations from marine and seabird sources at Ross Island, Antarctica, during AWARE. Atmos. Chem. Phys. 18, 8571–8587.
Lu, Z., Cai, M., Wang, J., Yang, H., He, J., 2012. Baseline values of metals in soils on fildes peninsula, King George Island, Antarctica: the extent of anthropogneic pollution. Environ. Monit. Assess. 184, 7013–7021.
Malaguti, A., Mircea, M., La Torretta, T.M.G., Telloli, C., Petralia, E., Stracquadanio, M., Barico, M., 2015. Chemical composition of fine and coarse aerosol particles in the central mediterranean area during dust and non-dust conditions. Aerosol Air Qual. Res. 15, 410–425.
Mayewski, P.A., Meredith, M.P., Summerhayes, C.P., Turner, J., Worby, A., co-authors, a., 2009. State of the Antarctic and southern ocean climate system. Rev. Geophys. 47, 1–30.
Mazzera, D.M., Lowenthal, D., Chow, J.C., Watson, J.G., Grubisic, V., 2001. PM_{10} measurements at McMurdo station, Antarctica Atmos. Environ. Times 35, 1891–1902.
Meskhidze, N., Nenes, A., 2006. Phytoplankton and cloudiness in the southern ocean. Science 314, 1419–1423.
Nriagu, J.O., 1979. Global inventory of natural and anthropogenic emissions of trace metals to the atmosphere. Nature 279, 409.
Nriagu, J.O., 1989. A global assessment of natural sources of atmospheric trace-metals. Nature 338, 47–49.
Nriagu, J.O., Pacyna, J.M., 1988. A global assessment of natural sources of atmospheric trace metals. Nature 33, 134.
Nylen, T.H., Fountain, A.G., Doran, P.T., 2004. Climatology of katabatic winds in the McMurdo dry valleys, southern Victoria Land, Antarctica. J. Geophys. Res. 109.
Pataud, J.P.e.a., 2010. A European aerosol phenomenology-3: physical and chemcial characteristics of particulate matter from 60 rural, urban, and kerside sites across Europe. Atmos. Environ. 44, 1308–1320.
Potapowicz, J., Szuminska, D., Szopinska, M., Polkowska, Z., 2019. The influence of global climate change on the environmental fate of anthropogenic pollution released from the permafrost Part I. Case study of Antarctica. Sci. Total Environ. 651, 1534–1548.
Quinn, P.K., Bates, T.S., 2011. The case against climate regulation via oceanic phytoplankton sulphur emissions. Nature 480, 51.
Querol, X., Alastuey, A., Rodriguez, S., Plana, F., Ruiz, C.R., Cots, N., Massagué, G., Puig, O., 2001. PM_{10} and $PM_{2.5}$ source apportionment in the barcelona metropolitan area, catalonia, Spain. Atmos. Environ 35, 6407–6419.
Ram, K., Sarin, M.M., 2010. Spatio-temporal variability in atmospheric abundances of EC, OC and WSOC over Northern India. J. Aerosol Sci. 41, 88–98.
Read, K.A., Lewis, A.C., Bauguitte, S., Rankin, A.M., Salmon, R.A., Wolff, E.W., Saiz-Lopez, A., Bloss, W.J., Heard, D.E., Lee, J.D., Plane, J.M.C., 2008. DMS and MSA measurements in the Antarctic Boundary Layer: impact of BrO on MSA production. Atmos. Chem. Phys. 8, 2985–2997.
Santos, I.R., Silva-Filho, E.V., Schaefer, C.E.G.R., Albuquerque-Filho, M.R., Campos, L.S., 2005. Heavy metal contamination in coastal sediments and soils near the Brazilian Antarctic station, King Goerge Island. Mar. Pollut. Bull. 50, 185–194.
Savoie, D.L., Prospero, J.M., 1989. Comparison of oceanic and continental sources of non-sea-salt sulphate over the Pacific Ocean. Nature 339, 685–687.
Seinfeld, J.H., Pandis, S.N., 2006. Atmospheric Chemistry and Physics: from Air Pollution to Climate Change, second ed. J. Wiley, New York.
Shaw, G.E., 1988. Antarctic aerosols: a review. Rev. Geophys. 26, 89–112.
Shi, G., Teng, J., Ma, H., Li, Y., Sun, B., 2015. Metals and metalloids in precipitation collected during CHINARE campaign from Shanghai, China to Zhongshan Station, Antarctica: spacial variability and source identification. Global Biogeochem. Cycles 29, 1–15.
Shi, G., Teng, J., Ma, H., Wang, D., Li, Y., 2018. Metals in topsil in Larsemann hills, an ice-free area in east antarctic: lithological and anthropogenic inputs. Catena 160, 41–49.
Signh, S.M., Nayaka, S., Upreti, D.K., 2007. Lichen communities in Larsemann hills, east Antarctica. Curr. Sci. India 93, 1670–1672.
Simon, H., Bhave, P.V., Swall, J.L., Frank, N.H., Malm, W.C., 2011. Determining the spatial and seasonal variability in OM/OC ratios across the US using multiple regression. Atmos. Chem. Phys. 11, 2933–2949.
Stull, R.B., 1988. An Introduction to Boundary Layer Meteorology. Springer Netherland, pp. 650–670.
Szopinska, M., Szuminska, D., Bialic, R.J., Chmiel, S., Plenzler, J., Polkowska, Z., 2018. Impact of newly-formed periglacial environment and other factors on fresh water chemistry at the western shore of admiralty Bay in summer of 2016 (King-George island, Maritime Antarctica). Sci. Total Environ. 613–614, 619–634.
Turpin, B.J., Lim, H.J., 2001. Species contributions to PM2.5 mass concentrations: revisiting common assumptions for estimating organic mass. Aerosol Sci. Technol. 35, 602–610.
van Lipzig, N.P.M., King, J.C., Lachlan-Cope, T.A., van der Broeke, M.R., 2004. Precipitation, sublimation and snow drift in the Antarctic peninsula region from a regional atmospheric model. J. Geophys. Res. 109, D24106.
Virkkula, A., Teinila, K., Hillamo, R., Kerminen, V.M., Saarikoski, S., Aurela, M., Viidanoja, J., Paatero, J., Koponen, I.K., Kulmala, M., 2006. Chemical composition of boundary layer aerosol over the Atlantic Ocean and at an Antarctic site. Atmos. Chem. Phys. 6, 3407–3421.
Wedepohl, K.H., 1995. The composition of the continental dust Geochim. Cosmochim. Acta 59, 1217–1232.
Weller, R., Wagenbach, D., 2007. Year-round chemical aerosol records in continental Antarctica obtained by automatic samplings, Tellus B: chemical and Physical Meteorology, 59 (4), 755–765.
Weller, R., Legrand, M., Preunkert, S., 2018. Size distribution and ionic composition of marine summer aerosol at the continental Antarctic site Kohnen. Atmos. Chem. Phys. 18, 2413–2430.
Weller, R., Wagenbach, D., Legrand, M., Elsasser, C., Tian-kunze, X., Konig-Langlo, G., 2011. Continuous 25-yr aerosol records at coastal Antarctica – I: inter-annual variability of ionic compounds and links to climate indices. Tellus 63B, 901–919.
Weller, R., Woltjen, J., Piel, C., Resenberg, R., Wagenbach, D., Konig-Langlo, G., al, e., 2008. Seasonal variability of crustal and marine trace elements in the aerosol at neumayer station, Antarctica. Tellus B 60, 742–752.
Wiggs, G., Baird, A., Atherton, R., 2004. The dynamic effects of moisture on ht entrainment and transport of sand by wind. Geomorphology 59, 13–30.
Xu, G., Chen, L., Zhang, M., Zhang, Y., Wang, J., Lin, Q., 2018. Year-round records of bulk aerosol composition over the zhongshan station, coastal east Antarctica. Air Qual. Atmosph. Health 12, 271–288.
Xu, Y., Ramanathan, V., Washington, W.M., 2016. Observed high-altitude warming and snow cover retreat over Tibet and the Himalayas enhanced by Black Carbon aerosols. Atmos. Chem. Phys. 16, 1303–1315.